protein in early hepatocellular carcinoma. Gastroenterology 2009;137:110–118.
[11] Inagaki Y, Tang W, Makuuchi M, Hasegawa K, Sugawara Y, Kokudo N. Clinical and molecular insights into the hepatocellular carcinoma tumour marker des-gamma-carboxyprothrombin. Liver Int 2011;31:22–35.
[12] Sheu JC, Sung JL, Chen DS, Lai MY, Wang TH, Yu JY, et al. Early detection of hepatocellular carcinoma by real-time ultrasonography. A prospective study. Cancer 1985;56:660–666.
[13] Collier J, Sherman M. Screening for hepatocellular carcinoma. Hepatology 1998;27:273–278.
[14] Schlattner U, Tokarska-Schlattner M, Wallimann T. Mitochondrial creatine kinase in human health and disease. Biochim Biophys Acta 2006;1762:164–180.
[15] Kanemitsu F, Kawanishi I, Mizushima J. A new creatine kinase found in mitochondrial extracts from malignant liver tissue. Clin Chim Acta 1983;128:233–240.
[16] Kanemitsu F, Kawanishi I, Mizushima J, Okigaki T. Mitochondrial creatine kinase as a tumor-associated marker. Clin Chim Acta 1984;138:175–183.
[17] Meffert G, Gellerich FN, Margreiter R, Wyss M. Elevated creatine kinase activity in primary hepatocellular carcinoma. BMC Gastroenterol 2005;5:9.
[18] Castaldo G, Salvatore F, Sacchetti L. Serum type-2 macro-creatine kinase isoenzyme is not a useful marker of severe liver diseases or neoplasia. Clin Biochem 1990;23:523–527.
[19] Hoshino T, Sakai Y, Yamashita K, Shirahase Y, Sakaguchi K, Asaeda A, et al. Development and performance of an enzyme immunoassay to detect creatine kinase isoenzyme MB activity using anti-mitochondrial creatine kinase monoclonal antibodies. Scand J Clin Lab Invest 2009;69:687–695.
[20] Makuuchi M, Kokudo N, Arii S, Futagawa S, Kaneko S, Kawasaki S, et al. Development of evidence-based clinical guidelines for the diagnosis and treatment of hepatocellular carcinoma in Japan. Hepatol Res 2008;38:37–51.
[21] Torzilli G, Minagawa M, Takayama T, Inoue K, Hui AM, Kubota K, et al. Accurate preoperative evaluation of liver mass lesions without fine-needle biopsy. Hepatology 1999;30:889–893.
[22] Omata M, Tateishi R, Yoshida H, Shiina S. Treatment of hepatocellular carcinoma by percutaneous tumor ablation methods: ethanol injection therapy and radiofrequency ablation. Gastroenterology 2004;127:S159–S166.
[23] Obi S, Yoshida H, Toune R, Unuma T, Kanda M, Sato S, et al. Combination therapy of intraarterial 5-fluorouracil and systemic interferon-alpha for advanced hepatocellular carcinoma with portal venous invasion. Cancer 2006;106:1990–1997.
[24] Wallimann T, Hemmer W. Creatine kinase in non-muscle tissues and cells. Mol Cell Biochem 1994;133–134:193–220.
[25] Vaubourdolle M, Chazouilleres O, Poupon R, Ballet F, Braunwald J, Legendre C, et al. Creatine kinase-BB: a marker of liver sinusoidal damage in ischemia-reperfusion. Hepatology 1993;17:423–428.
[26] Stein W, Bohner J, Bahlinger M. Analytical patterns and biochemical properties of macro creatine kinase type 2. Clin Chem 1985;31:1952–1958.
[27] Lee KN, Csako G, Bernhardt P, Elin RJ. Relevance of macro creatine kinase type 1 and type 2 isoenzymes to laboratory and clinical data. Clin Chem 1994;40:1278–1283.
[28] Schmid H, Muhlbayer D, Roling J, Sternfeld T, Julg B, Schlattner U, et al. Macroenzyme creatine kinase (CK) type 2 in HIV-infected patients is significantly associated with TDF and consists of ubiquitous mitochondrial CK. Antivir Ther 2006;11:1071–1080.
[29] Hatano E, Tanaka A, Kanazawa A, Tsuyuki S, Tsunekawa S, Iwata S, et al. Inhibition of tumor necrosis factor-induced apoptosis in transgenic mouse liver expressing creatine kinase. Liver Int 2004;24:384–393.
[30] Miller K, Halow J, Koretsky AP. Phosphocreatine protects transgenic mouse liver expressing creatine kinase from hypoxia and ischemia. Am J Physiol 1993;265:C1544–C1551.
[31] Hatano E, Tanaka A, Iwata S, Satoh S, Kitai T, Tsunekawa S, et al. Induction of endotoxin tolerance in transgenic mouse liver expressing creatine kinase. Hepatology 1996;24:663–669.
[32] Miller K, Sharer K, Suhan J, Koretsky AP. Expression of functional mitochondrial creatine kinase in liver of transgenic mice. Am J Physiol 1997;272:C1193–C1202.
[33] Dolder M, Walzel B, Speer O, Schlattner U, Wallimann T. Inhibition of the mitochondrial permeability transition by creatine kinase substrates. Requirement for microcompartmentation. J Biol Chem 2003;278:17760–17766.
[34] Kanemitsu F, Mizushima J, Kageoka T, Okigaki T, Taketa K, Kira S. Characterization of two types of mitochondrial creatine kinase isolated from normal human cardiac muscle and brain tissue. Electrophoresis 2000;21:266–270.
[35] Malhi H, Gores GJ. Cellular and molecular mechanisms of liver injury. Gastroenterology 2008;134:1641–1654.
[36] Friedman SL. Mechanisms of hepatic fibrogenesis. Gastroenterology 2008;134:1655–1669.

Biochemical and Biophysical Research Communications 420 (2012) 564–569

Contents lists available at SciVerse ScienceDirect

Biochemical and Biophysical Research Communications

journal homepage: www.elsevier.com/locate/ybbrc

A miRNA machinery component DDX20 controls NF-κB via microRNA-140 function

Akemi Takata, Motoyuki Otsuka *, Takeshi Yoshikawa, Takahiro Kishikawa, Yotaro Kudo, Tadashi Goto, Haruhiko Yoshida, Kazuhiko Koike

Department of Gastroenterology, Graduate School of Medicine, The University of Tokyo, Tokyo 113-8655, Japan

ARTICLE INFO

Article history:
Received 28 February 2012
Available online 16 March 2012

Keywords:
DDX20
NF-κB
MicroRNA

ABSTRACT

Hepatocellular carcinoma is the third leading cause of cancer mortality worldwide, but the molecular mechanisms in tumorigenesis remain largely unknown. Previously, a DEAD-box protein DDX20, a component of microRNA-containing ribonucleoprotein complexes, was identified as a liver tumor suppressor candidate in an oncogenomics-based *in vivo* RNAi screen. However, the molecular mechanisms were unknown. Here, we show that deficiency of DDX20 results in the enhancement of NF-κB activity, a crucial intracellular signaling pathway closely linked with hepatocarcinogenesis. While DDX20 normally suppresses NF-κB activity by regulating NF-κB-suppressing miRNA-140 function, this suppressive effect was lost in DDX20-deficient cells. The impairment of miRNA function due to DDX20 deficiency appears to be miRNA species-specific at the point of loading miRNAs into the RNA-induced silencing complex. These results indicate that DDX20 deficiency enhances NF-κB activity by impairing the NF-κB-suppressive action of microRNAs, and suggest that dysregulation of the microRNA machinery components may also be involved in pathogenesis in various human diseases.

1. Introduction

The incidence of hepatocellular carcinoma, the third most common cause of cancer-related mortality worldwide [1], is increasing in Western countries [2]. While numerous studies have investigated molecular abnormalities in hepatocarcinogenesis, the development of this disease cannot be attributed to any single oncogenic event. Thus, drugs targeting various molecular pathways must be evaluated in combination with, or in comparison with, the current therapeutic options [3]. Although recent findings on the effectiveness of sorafenib, a multi-kinase inhibitor, are promising, the survival benefit is only less than 3 months [4]. As no effective therapy currently exists, a better understanding of the exact mechanisms involved in hepatocarcinogenesis remains the fundamental foundation for developing new candidate drugs.

DDX20 (also known as Gemin3 or DP103) was originally isolated as a DEAD-box protein that associated with the Epstein–Barr virus nuclear proteins EBNA2 and EBNA3C [5]. This protein has also been isolated independently as an interactant of survival motor neuron protein (SMN) in the gems, and in cytoplasmic spliceosomal small nuclear ribonucleoprotein complexes (snRNPs) [6]. These results suggest that DDX20 is involved in both transcriptional regulation and RNA processing. More evidence has indicated that DDX20 acts as a transcriptional regulator [7–9]. Concurrently, DDX20 was identified as a major component of microRNA (miRNA)-containing ribonucleoprotein complexes (miRNPs) that also contain eIF2C2 (Argonaute 2; Ago2) [10,11], and which perform translational control in the miRNA pathway. In addition, attempts to create DDX20 knockout mice have resulted in embryonic lethality, suggesting that this protein has essential biologic roles [12].

Recently, an oncogenomics-based *in vivo* RNAi screen identified 13 new tumor-suppressor genes in murine liver cancers [13], one of which was DDX20. Because DDX20 has not been clearly linked to liver cancer previously, the molecular mechanisms by which the dysregulation of this gene causes hepatocellular carcinoma are unknown. To address these, we examined the deregulated intracellular signaling pathway caused by DDX20 deficiency and identified a previously unknown intracellular signaling pathway.

2. Methods

2.1. Cell culture

PLC/PRF/5, Huh7, and 293T cells were maintained in Dulbecco's modified Eagle's medium (DMEM) supplemented with 10% fetal bovine serum (FBS). Hep3B cells were cultured in DMEM supplemented with 10% nonessential amino acids and 10% FBS.

* Corresponding author. Address: Department of Gastroenterology, Graduate School of Medicine, The University of Tokyo, 7-3-1 Hongo, Bunkyo-ku, Tokyo 113-8655, Japan. Fax: +81 3 3814 0021.
E-mail address: otsukamo-tky@umin.ac.jp (M. Otsuka).

0006-291X/$ - see front matter © 2012 Elsevier Inc. All rights reserved.
http://dx.doi.org/10.1016/j.bbrc.2012.03.034

2.2. Plasmids

FLAG-tagged human DDX20-expressing plasmids were kindly provided by Dr. C. Glass and Dr. G. Dreyfuss [8,10]. FLAG-tagged human DDX20-expression plasmids used for generation of DDX20-overexpressing lentiviruses were constructed by inserting the PCR-amplified DDX20 cDNA at the NotI site of the pCDH vector (System Biosciences). Plasmids expressing microRNA precursors (miRNA-22 and miRNA-140 precursors) were purchased from System Biosciences (Mountain View, CA). Reporter plasmids to analyze miRNA function were constructed by inserting annealed synthetic primers containing two tandem sequences, complementary to each miRNA, into the 3′-UTR of the firefly luciferase gene, driven by the CMV promoter (pGL3-basic; Promega, Madison, WI), at the FseI site. Primers used for PCR amplification of DDX20 were: forward, 5′-GCG GCC GCG CCG CCA TGG ACT ACA AGG ACG ACG ACG ACA AGG ACT ACA AGG ACG ACG ACG ACA AGA TGG CGG CGG CAT TTG AAG C-3′ and reverse, 5′-GCG GCC GCT CAC TGG TTA CTA TGC ATC AT TTC-3′. The sequences of the primers used for reporter plasmid construction were as follows: miR-22, 5′-ACA GTT CTT CAA CTG GCA GCT TAA TTA CAG TTC TTC AAC TGG CAG CTT CTC GAG CCG G-3′; miRNA-140–3p, 5′-CCG TGG TTC TAC CCT GTG GTA AAT TCC GTG GTT CTA CCC TGT GGT ACT CGA GCC GG-3′; miRNA-140-5p, 5′-CTA CCA TAG GGT AAA ACC ACT GAA TTC TAC CAT AGG GTA AAA CCA CTG CTC GAG CCG G-3′.

2.3. Lentiviral production and transduction

Cells were transduced with DDX20 (Gemin3)-shRNA and control-shRNA lentiviral particles (Santa Cruz Biotechnology) and then selected on puromycin. To produce FLAG-tagged DDX20 expressing-lentiviruses, 293T cells were transfected with pPACKH1 Packaging Plasmid Mix (System Biosciences) and pCDH-FLAG-tagged DDX20 expressing-lentivector constructs. After 2 days, the supernatants were collected and the viruses were concentrated using PEG-it Virus Precipitation Solution (System Biosciences).

2.4. Transfection and luciferase assay

Transfection was performed using Fugene6 (Promega). Luciferase activities were measured by use of a Dual Luciferase Reporter Assay System (Promega) as described previously [14].

2.5. RNA isolation and reverse transcription

Total RNA was isolated using Trizol Reagent (Invitrogen, Carlsbad, CA). cDNA was synthesized from RNA using the SuperScript III First-Strand Synthesis System (Invitrogen).

2.6. Antibodies

The following antibodies were used: mouse anti-Gemin3 (Ddx20) (sc-57007), rabbit anti-TRADD (sc-7868), rabbit anti-RIP (sc-7881), mouse anti-IKKα (sc-7183), mouse anti-NF-κB p65 (sc-8008), and mouse anti-NF-κB p50 (sc-7188), all purchased from Santa Cruz Biotechnology (Santa Cruz, CA); mouse anti-β-actin (A5316), purchased from Sigma (St. Louis, MO); mouse anti-TRAF2 (#558890) and mouse anti-IKKγ (#559675), purchased from BD Pharmingen (San Diego, CA); rabbit anti-TAK1 (#4505) and rabbit anti-IKKβ (#2370), purchased from Cell Signaling Technology (Danvers, MA); mouse anti-IκBα (#610690), purchased from BD Transduction Laboratories (Lexington, KY); mouse anti-Ago2 (#015-22031) and mouse anti-DYKDDDDY (FLAG)-tag (#018-22381), purchased from Wako (Osaka, Japan).

2.7. Western blotting

Western blotting was performed as described previously [15].

2.8. Reporter plasmids for signal transduction

The following reporter plasmids were used to examine how DDX20 modulated intracellular signaling: pNF-κB-luc, pGAS (IFNγ-activated sequences)-luc, pSRE-luc, pAP-1-luc, and p53-luc were purchased from Stratagene (La Jolla, CA). IL-8-luc, and p3TP-luc (to determine TGFβ pathway activity), were described previously [16]. To construct a reporter plasmid containing mutated NF-κB binding sites, the NF-κB binding motifs, GGGAATTTCC, in pNF-κB-luc were mutated to ATCAATTTCA, as previously reported [17]. Synthetic oligonucleotides with four mutant binding sites (forward, 5′-CTA GCA TCA ATT TCA ATC AAT TTC AAT CAA TTT CAA TCA ATT TCA A-3′; reverse, 5′-GAT CTT GAA ATT GAT TGA AAT TGA TTG AAA TTG ATT GAA ATT GAT G-3′) were annealed and cloned into the NheI and BglII sites of pNF-κB-luc to replace the original NF-κB binding motifs. As positive controls, the following were used: transfection with pFC-MEKK, a MEKK-expressing plasmid, for NF-κB-luc, SRE-luc, and AP-1-luc; transfection with p53-expressing plasmid for p53-luc; incubation for 6 h with 5 ng/mL IFNγ (ProSpec-Tany TechnoGene, Rehovot, Israel) for GAS-luc, and with 5 ng/mL TGFβ (Peprotech, Rocky Hill, NJ) for p3TP-luc.

2.9. EMSA

Nuclear extracts were prepared as described previously [18]. Five micrograms of nuclear extract were incubated with a double-stranded biotin-labeled DNA probe containing NF-κB binding sites (5′-AGT TGA GGG GAC TTT CCC AGG C-3′) plus 1 μg of poly (dI-dC) in a binding buffer (50 mM Tris [pH 7.5], 250 mM NaCl, 2.5 mM DTT, 2.5 mM EDTA, 5 mM $MgCl_2$, and 20% glycerol) at 15 °C for 30 min. DNA–protein complexes were separated on a 6% non-denaturing polyacrylamide gel in 0.5x TBE, and then transferred to nylon membrane (Hybond-N^+; GE Healthcare Life Sciences). Oligonucleotides were visualized using the LightShift Chemiluminescent EMSA Kit (Thermo Scientific, Rockford, IL). DNA–protein complex specificity was tested by adding a 100-fold excess of unlabeled (cold) NF-κB probe. To confirm equal loading of nuclear-extracts, the amounts of TFIID, a nuclear protein, were examined by Western blotting using an anti-TFIID antibody (sc-273; Santa Cruz).

2.10. miRNA isolation and quantitation

To measure the amounts of different microRNAs in cells, a Mir-X miRNA qRT-PCR SYBR Kit (Clontech, Mountain View, CA) was used. The levels of U6 snRNA were used for the normalization of cellular miRNA levels. To purify miRNAs from Ago2-related RISCs and DDX20-associated miRNP complexes, microRNAs fractions were isolated using the Human Ago2 MicroRNA Isolation Kit (Wako, Osaka, Japan), which uses antibodies raised to Ago2 and DDX20 to precipitate miRNAs from Ago2-related RISCs and DDX20-associated miRNPs, respectively. The primers used in the quantitative PCR analysis for miRNAs were miRNA-140-5p, CAG TGG TTT TAC CCT ATG GTA G; miRNA-140-3p, TAC CAC AGG GTA GAA CCA CGG; miRNA-22, AAG CTG CCA GTT GAA GAA CTG T.

2.11. Quantitative PCR

Quantitative PCR was performed using the TaqMan Gene Expression system and SYBR Green (Applied Biosystems, Foster City, CA). All target gene expression values were normalized to the expression values for the housekeeping gene, GAPDH, and

relative expression levels were calculated by the $\Delta\Delta C_T$ method: $\Delta\Delta C_T = \Delta C_{Tsample} - \Delta C_{Tgapdh}$ The primers used included (5′–3′): IL-6 forward, CAC AGA CAG CCA CTC ACC TC; IL-6 reverse, TTT TCT GCC AGT GCC TCT TT; IL-8 forward, ATG ACT TCC AAG CTG GCC GTG GCT; IL-8 reverse, TCT CAG CCC TCT TCA AAA ACT TCT C; GAPDH forward, ATC AAC GAC CCC TTC ATT GAC C, and GAPDH reverse, CCA GTA GAC TCC ACG ACA TAC TCA GC.

2.12. Immunoprecipitation

For immunoprecipitation, 293T cells were transfected with FLAG-tagged DDX20-expressing plasmids. FLAG-tagged DDX20 protein was precipitated by incubation with anti-FLAG M2 agarose (Sigma) for 8 h. Cell extracts were prepared as described previously [16].

2.13. Statistical analysis

Statistically significant differences were determined using Student's *t*-test, when variances were equal. When variances were unequal, Welch's *t*-test was instead used.

3. Results

3.1. DDX20 modulates the NF-κB activity

Because it was reported that DDX20 regulates transcriptions [7–9,19], we first examined the effects of altered DDX20 levels on intracellular signaling pathways by a reporter assay (Fig. 1A). While SRE was repressed moderately by DDX20 overexpression consistent with a previous report (Fig. 1A) [8], NF-κB activity was also decreased significantly in our study (Fig. 1A). Thus, we next examined NF-κB activity in stable DDX20-knockdown PLC/PRF/5 cells (Fig. 1B). Whereas DDX20-knockdown cells showed slightly higher NF-κB activity than control cells (Fig. 1C), the response was significantly enhanced by TNFα, which induces NF-κB activity and is involved in the pathogenesis of hepatitis, leading to HCC [20–23] (Fig. 1C). DDX20-knockdown cells consistently showed significantly higher promoter activity for the interleukin (IL)-8 gene, a gene known to be induced by NF-κB [24] (Fig. 1D). To exclude the possibility of cell-specific effects, we established DDX20-knockdown Huh7 cells and observed a similar trend in these cell lines (Supplementary Fig. S1a, b, and c). To further confirm these findings in an overexpression model, we established FLAG-tagged DDX20-overexpressing stable cell lines (Supplementary Fig. S2a). Restoration of NF-κB activity and mRNA levels of IL-6 and IL-8 resulted from DDX20 overexpression, consistent with the results from DDX20-knockdown cells (Supplementary Fig. S2b and c). These results also suggest that DDX20 normally functions to suppress NF-κB activity and the resulting downstream effects of this pathway.

3.2. DDX20 does not modulate or interact with molecules in the NF-κB canonical pathway

To determine how DDX20 deficiency enhances NF-κB activity, we examined the DNA-binding activity of NF-κB, which was increased in DDX20-knockdown cells (Fig. 2A). Although we

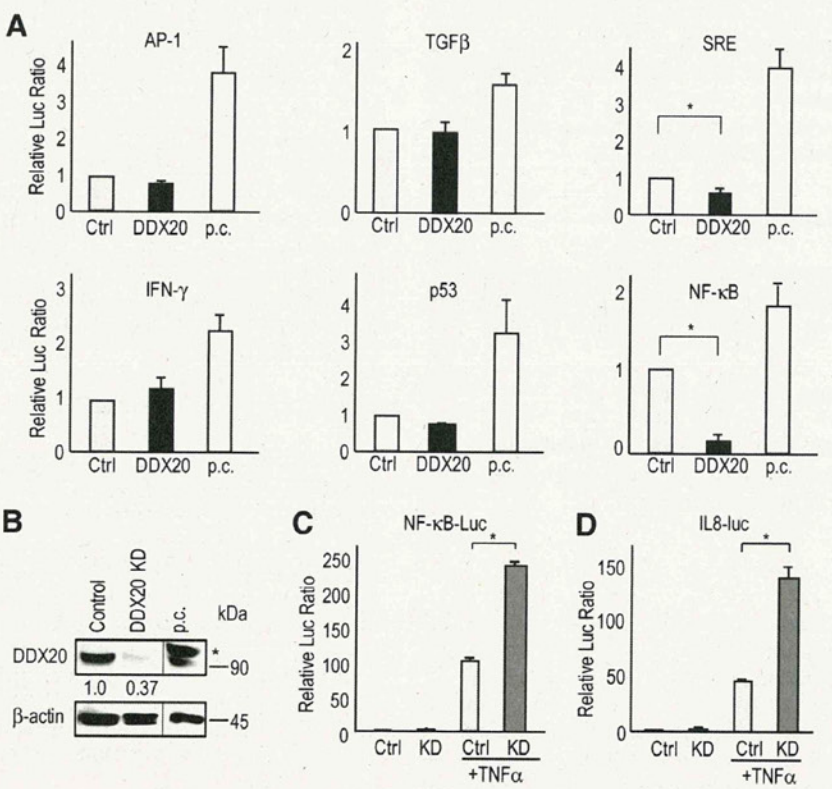

Fig. 1. Modulation of the NF-κB pathway by DDX20. (A) The effects of DDX20 on intracellular signaling pathways as assessed by a reporter assay. Huh7 cells were transiently transfected with a luciferase reporter plasmid and a DDX20-expressing (DDX20) or control plasmid (Ctrl). Luciferase values from control cells were set to 1. The data shown represent the means ± s.d. from at least four independent experiments. p.c.; positive control. (B) Establishment of stable DDX20-knockdown PLC/PRF/5 cells. *FLAG-tagged human DDX20 as a positive control (p.c.). (C, D) Reporter assay data showing that DDX20 deficiency enhances the TNFα-induced activity of NF-κB. Reporter plasmids for NF-κB (C) and its target gene, IL-8 (D), were transiently transfected into control (Ctrl) or DDX20-knockdown (KD) cells. The cells were treated with TNFα (5 ng/mL) or vehicle for 6 h before the reporter assay was performed. *$p < 0.05$. The data shown represent the means ± s.d. from three independent experimental trials. Similar results were obtained in DDX20-knockdown Huh7 cells.

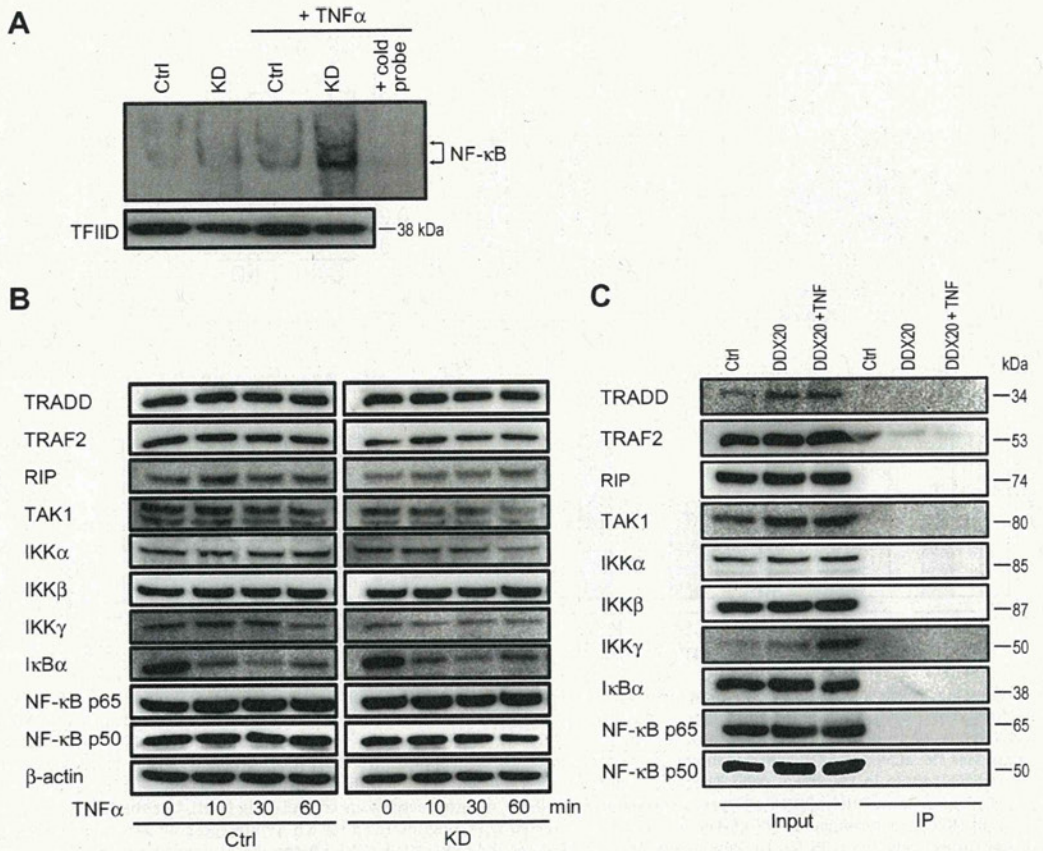

Fig. 2. NF-κB DNA binding is increased in DDX20 knockdown cells after TNFα stimulation. (A) Nuclear extracts from unstimulated and TNFα-stimulated control (Ctrl) and DDX20-knockdown (KD) PLC/PRF/5 cells were analyzed by electrophoretic mobility-shift assay. The specificity of the DNA–protein complex was tested by adding unlabeled NF-κB probe (cold probe) to the TNFα-stimulated KD nuclear extracts. TFIID amounts were examined to confirm equal nuclear extract loading. A representative result is shown from four independent experiments. Similar results were obtained using Huh7 cells. (B) Control (Ctrl) and DDX20-knockdown (KD) PLC/PRF/5 cells were stimulated with 5 ng/mL TNFα for the times indicated. Western blotting was performed using antibodies against the indicated proteins. A representative result is shown from two independent experiments. Similar results were obtained using Huh7 cells. (C) 293T cells (treated with or without 5 ng/mL TNFα for 6 h before the assay) were transfected with a control vector (Ctrl) or a FLAG-tagged DDX20-expressing (DDX20) plasmid. FLAG-tagged DDX20 was immunoprecipitated using anti-FLAG agarose. Co-precipitated proteins were blotted using antibodies against the indicated proteins. Five percent of the total cell lysates were loaded as an input control. Representative results from two independent experiments are shown.

observed IκB-α protein degradation after TNFα stimulation, as expected, the degree of degradation was similar in the control and DDX20-knockdown cells (Fig. 2B) and the levels of the other proteins examined were also similar (Fig. 2B). In addition, we were unable to detect any interactions between DDX20 and the NF-κB pathway-related molecules examined (Fig. 2C). These results suggest that it is unlikely that DDX20 modulates NF-κB activity either by interacting directly with these molecules or by altering their expression levels.

3.3. DDX20 deficiency enhances NF-κB activity by impairing miRNA-140-3p function

Because DDX20 interacts with Ago2 (Fig. 3A), which plays a central role in miRNA function [10,11], we hypothesized that DDX20 deficiency leads to impaired miRNA function and to subsequent activation of NF-κB. Because we previously identified by a comprehensive liver-expressing miRNA library screen that miRNA-22 and miRNA-140 are the critical suppressors of NF-κB activities [25], we hypothesized that DDX20 deficiency enhances NF-κB activity by impairing the NF-κB-suppressing miRNA function.

In DDX20-knockdown cells, the effects of miRNA-140-3p were reduced significantly (Fig. 3B). This impairment of miRNA function had miRNA species-specificity because the degree of functional impairment in DDX20-knockdown cells was much greater for miRNA-140-3p than for miRNA-140-5p and miRNA-22 (Fig. 3B).

While miRNA-22 and miRNA-140 suppressed NF-κB activity in the control cells as we previously reported [25] (Fig. 3C), the suppressive effects of miRNA-140 on NF-κB activity were reduced significantly in DDX20-knockdown cells (Fig. 3C). The reversal of the suppressive effect of miRNA-140 appeared to depend on miRNA-140-3p as miRNA-140-5p showed less functional impairment than did miRNA-140-3p when the corresponding reporter constructs were used as described above (Fig. 3B). The effect was NF-κB specific because no effects were observed for reporters with mutations in the NF-κB binding sites (Fig. 3D).

3.4. DDX20 preferentially interacts with miRNA-140-3p

To elucidate the mechanisms by which DDX20 preferentially impairs certain miRNA functions, we compared the levels of mature miRNAs (miR-22, 140-3p, and 140-5p) in control cells and in DDX20-knockdown cells and found them to be comparable (Fig. 4A). This suggests that DDX20 was not involved in miRNA maturation. We next considered the possibility that the preferential impairment of miRNA function in DDX20-knockdown cells was caused by preferential loading of miRNAs into the RNA-induced silencing complex (RISC). To test this, we immunoprecipitated

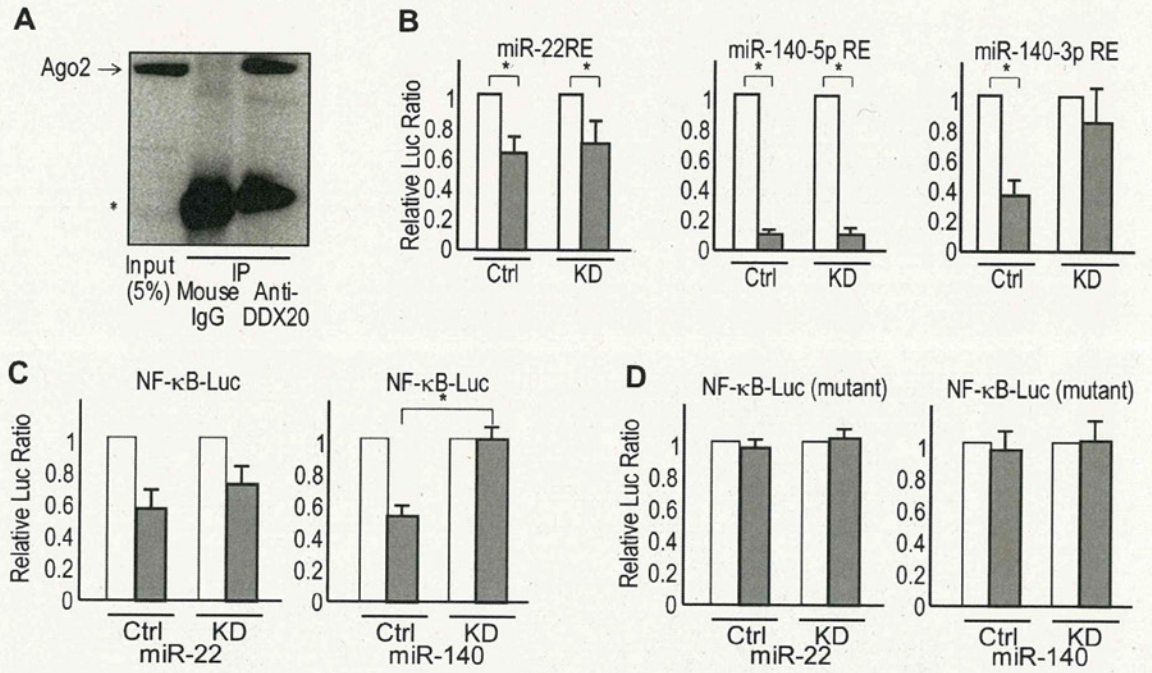

Fig. 3. DDX20 deficiency enhances NF-κB activity by impairing miRNA function. (A) DDX20 binds Ago2. 293T cells were transfected with a FLAG-tagged DDX20-expressing plasmid, and immunoprecipitated using monoclonal antibodies against FLAG-tag or non-immune mouse IgG. Precipitates were blotted with a human anti-Ago2 antibody. Five per cent of each cell lysate was used as an "input" to show the endogenous Ago2 protein. *Bands derived from immunoglobulin light-chain. (B) Overexpression of the miRNA precursors suppresses the activities of the corresponding promoter-reporter constructs in control cells (Ctrl), whereas DDX20 knockdown (DDX KD) reverses the suppressive effects of miRNA-140-3p in PLC/PRF/5 cells. The white and gray bars indicate results with the empty vector and with miRNA precursor overexpression, respectively. $^*p < 0.05$. (C) Expression of the miRNA-140 precursor suppresses NF-κB reporter activity in control cells (Ctrl), but this effect was attenuated in DDX20-knockdown PLC/PRF/5 cells (KD) as determined by NF-κB-Luc. The cells were treated with 5 ng/mL TNFα for 6 h. White and gray bars indicate empty vector and miRNA precursor overexpression, respectively. $^*p < 0.05$. (D) The suppressive effects by miR-22 and miR-140 were NF-κB-specific. Mutant NF-κB reporter plasmids were transfected with an empty vector (white bar) or the corresponding miRNA precursor-expression plasmids (black bar), into control (Ctrl) and DDX20-knockdown (KD) PLC/PRF/5 cells. Data were normalized and represent the mean ± s.d. of three independent experiments. Similar results were obtained using DDX20-knockdown Huh7 cells.

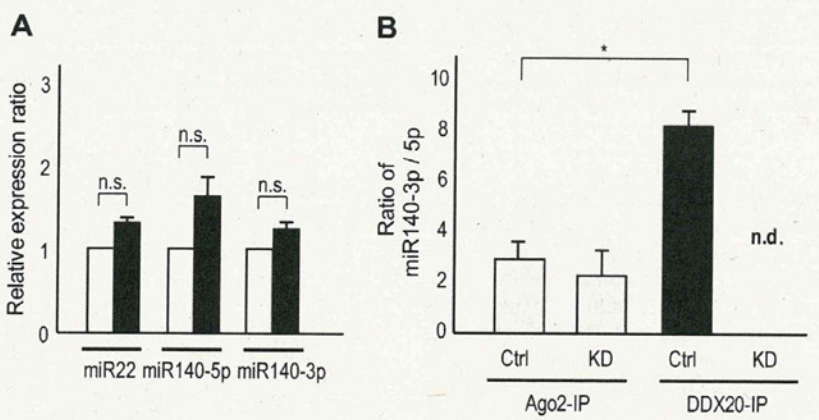

Fig. 4. DDX20 preferentially interacts with miRNA-140-3p. (A) Relative expression of indicated mature miRNAs in the total cellular RNA were measured and normalized to the level of U6 snRNA. The relative ratios of the miRNAs in control cells (white bars) and DDX20-knockdown cells (black bars) were calculated. The data represent the means ± s.d. of six independent experiments. n.s.; non significant. (B) The ratios of miRNA-140-3p to miRNA-140-5p in Ago2- and DDX20-associated RISCs as determined from anti-Ago2 or anti-DDX20 immunoprecipitates (IP) in PLC/PRF/5 control (Ctrl) and DDX20-knockdown (KD) cells. The ratios shown are the means ± s.d. of six independent experiments. Because DDX20-knockdown cells are deficient in DDX20, the anti-DDX20 miRNA ratio was not determined in these cells (n.d.).

Ago2-related RISCs and measured the amount of different miRNAs in the complexes. Because there are no standard small RNAs that can be used as a "house-keeping gene" to adjust for variation in sample loading, we compared miRNA140-5p:miRNA140-3p ratios (since both miRNAs are derived from a single precursor). This ratio in Ago2-related RISCs was approximately two in both control and DDX20-knockdown cells, suggesting that DDX20 was not involved in the preferential loading of specific miRNAs into Ago2-related RISCs (Fig. 4B). However, the ratio in the DDX20-associated miRNPs precipitated from control cells was approximately one to eight (Fig. 4B), indicating that DDX20 preferentially interacts with certain miRNAs, such as miRNA-140-3p, in DDX20-associated miRNPs. The results suggest that functional impairment of certain miRNAs in DDX20-knockdown cells might be caused by the preferential loading of certain miRNAs into DDX20-associated miRNPs. These results further suggest that DDX20 deficiency impairs the function of certain subsets of miRNAs and that this impairment could enhance NF-κB activity by deregulating the NF-κB-suppressive actions of miRNAs, especially miRNA-140-3p, in DDX20-deficient cells.

4. Discussion

Here we report that DDX20 deficiency may enhance NF-κB activities through impairing the NF-κB-suppressing miRNA-140 functions. It was reported that DDX20 is a possible liver tumor suppressor in mice [13]. NF-κB activation is a common feature of human HCCs, particularly those linked to hepatitis [26,27]. In fact, experiments using patient samples suggest that NF-κB activation in the liver leads to the development of HCC [28]. Taken together, these results suggest that the enhancement of NF-κB activity that occurs when DDX20 is deficient may play a role on hepatocarcinogenesis.

Our results indicate that, although DDX20 is one of the major components of Ago2-related RISCs, which play central roles in global miRNA functions [10], impairment of miRNA function due to DDX20 deficiency appears to be miRNA species-specific at the point of loading miRNAs into RISCs. While the precise mechanisms how DDX20 preferentially loads specific miRNAs into RISCs remain to be elucidated, because not all miRNPs have the same components, variation in RISC complexes may determine the properties or specificities of individual miRNAs [10].

Because DDX20 is a multifunctional protein, the miRNA functional impairment reported in the present study may not be the only consequence of DDX20 deficiency. In addition, because novel miRNAs are continually being discovered, other currently unknown miRNAs may also be involved in the biologic role of DDX20. Nonetheless, this study shows that DDX20 is involved in the function of specific miRNAs and the resulting control of NF-κB activity. These results suggest that it is important to investigate not only aberrant miRNA expression levels [29–32] but also deregulation of miRNP components with the subsequent impairment of miRNA function as a path of pathogenesis in human diseases.

Acknowledgments

We thank G. Dreyfuss, and C.K. Glass for providing materials. This work was supported by Grants-in-Aid from the Ministry of Education, Culture, Sports, Science and Technology, Japan (#22390058, #23590960, #17016016, and #20390204) (M. Otsuka, T.G., M. Omata, and K. Koike); by Health Sciences Research Grants from the Ministry of Health, Labor and Welfare of Japan (Research on Hepatitis) (to K. Koike).

Appendix A. Supplementary data

Supplementary data associated with this article can be found, in the online version, at http://dx.doi.org/10.1016/j.bbrc.2012.03.034.

References

[1] D. Parkin, F. Bray, J. Ferlay, P. Pisani, Global cancer statistics, 2002, CA Cancer. J. Clin. 55 (2005) 74–108.
[2] H. El-Serag, Epidemiology of hepatocellular carcinoma in USA, Hepatol. Res. 37 (Suppl.2) (2007) S88–94.
[3] J. Llovet, J. Bruix, Molecular targeted therapies in hepatocellular carcinoma, Hepatology 48 (2008) 1312–1327.
[4] J. Llovet, S. Ricci, V. Mazzaferro, P. Hilgard, E. Gane, J. Blanc, A. de Oliveira, A. Santoro, J. Raoul, A. Forner, M. Schwartz, C. Porta, S. Zeuzem, L. Bolondi, T. Greten, P. Galle, J. Seitz, I. Borbath, D. Häussinger, T. Giannaris, M. Shan, M. Moscovici, D. Voliotis, J. Bruix, S.I.S. Group, Sorafenib in advanced hepatocellular carcinoma, N. Engl. J. Med. 359 (2008) 378–390.
[5] M. Voss, A. Hille, S. Barth, A. Spurk, F. Hennrich, D. Holzer, N. Mueller-Lantzsch, E. Kremmer, F. Grässer, Functional cooperation of Epstein-Barr virus nuclear antigen 2 and the survival motor neuron protein in transactivation of the viral LMP1 promoter, J. Virol. 75 (2001) 11781–11790.
[6] B. Charroux, L. Pellizzoni, R. Perkinson, A. Shevchenko, M. Mann, G. Dreyfuss, Gemin3: a novel DEAD box protein that interacts with SMN, the spinal muscular atrophy gene product, and is a component of gems, J. Cell. Biol. 147 (1999) 1181–1194.
[7] Q. Ou, J. Mouillet, X. Yan, C. Dorn, P. Crawford, Y. Sadovsky, The DEAD box protein DP103 is a regulator of steroidogenic factor-1, Mol. Endocrinol. 15 (2001) 69–79.
[8] G. Klappacher, V. Lunyak, D. Sykes, D. Sawka-Verhelle, J. Sage, G. Brard, S. Ngo, D. Gangadharan, T. Jacks, M. Kamps, D. Rose, M. Rosenfeld, C. Glass, An induced Ets repressor complex regulates growth arrest during terminal macrophage differentiation, Cell 109 (2002) 169–180.
[9] A. Gillian, J. Svaren, The Ddx20/DP103 dead box protein represses transcriptional activation by Egr2/Krox-20, J. Biol. Chem. 279 (2004) 9056–9063.
[10] Z. Mourelatos, J. Dostie, S. Paushkin, A. Sharma, B. Charroux, L. Abel, J. Rappsilber, M. Mann, G. Dreyfuss, MiRNPs: a novel class of ribonucleoproteins containing numerous microRNAs, Genes Dev. 16 (2002) 720–728.
[11] G. Hutvágner, P. Zamore, A MicroRNA in a multiple-turnover RNAi enzyme complex, Science 297 (2002) 2056–2060.
[12] J. Mouillet, X. Yan, Q. Ou, L. Jin, L. Muglia, P. Crawford, Y. Sadovsky, DEAD-box protein-103 (DP103, Ddx20) is essential for early embryonic development and modulates ovarian morphology and function, Endocrinology 149 (2008) 2168–2175.
[13] L. Zender, W. Xue, J. Zuber, C. Semighini, A. Krasnitz, B. Ma, P. Zender, S. Kubicka, J. Luk, P. Schirmacher, W. McCombie, M. Wigler, J. Hicks, G. Hannon, S. Powers, S. Lowe, An oncogenomics-based in vivo RNAi screen identifies tumor suppressors in liver cancer, Cell 135 (2008) 852–864.
[14] M. Otsuka, Q. Jing, P. Georgel, L. New, J. Chen, J. Mols, Y.J. Kang, Z. Jiang, X. Du, R. Cook, S.C. Das, A.K. Pattnaik, B. Beutler, J. Han, Hypersusceptibility to vesicular stomatitis virus infection in Dicer1-deficient mice is due to impaired miR24 and miR93 expression, Immunity 27 (2007) 123–134.
[15] M. Otsuka, A. Takata, T. Yoshikawa, K. Kojima, T. Kishikawa, C. Shibata, M. Takekawa, H. Yoshida, M. Omata, K. Koike, Receptor for activated protein kinase C: requirement for efficient microRNA function and reduced expression in hepatocellular carcinoma, PLoS One 6 (2011) e24359.
[16] M. Otsuka, N. Kato, K. Lan, H. Yoshida, J. Kato, T. Goto, Y. Shiratori, M. Omata, Hepatitis C virus core protein enhances p53 function through augmentation of DNA binding affinity and transcriptional ability, J. Biol. Chem. 275 (2000) 34122–34130.
[17] J. Miyagawa, M. Muguruma, H. Aoto, I. Suetake, M. Nakamura, S. Tajima, Isolation of the novel cDNA of a gene of which expression is induced by a demethylating stimulus, Gene (1999) 289–295.
[18] E. Schreiber, P. Matthias, M. Müller, W. Schaffner, Rapid detection of octamer binding proteins with 'mini-extracts', prepared from a small number of cells, Nucleic Acids Res. 17 (1989) 6419.
[19] F. Fuller-Pace, A. Jacobs, S. Nicol, Modulation of transcriptional activity of the DEAD-box family of RNA helicases, p68 (Ddx5) and DP103 (Ddx20), by SUMO modification, Biochem. Soc. Trans. 35 (2007) 1427–1429.
[20] T. Luedde, R.F. Schwabe, NF-κB in the liver–linking injury, fibrosis and hepatocellular carcinoma, Nat. Rev. Gastroenterol. Hepatol. 8 (2011) 108–118.
[21] M. Arsura, L. Cavin, Nuclear factor-kappaB and liver carcinogenesis, Cancer Lett. 229 (2005) 157–169.
[22] E. Pikarsky, R. Porat, I. Stein, R. Abramovitch, S. Amit, S. Kasem, E. Gutkovich-Pyest, S. Urieli-Shoval, E. Galun, Y. Ben-Neriah, NF-kappaB functions as a tumour promoter in inflammation-associated cancer, Nature 431 (2004) 461–466.
[23] D. Tai, S. Tsai, Y. Chang, S. Huang, T. Chen, K. Chang, Y. Liaw, Constitutive activation of nuclear factor kappaB in hepatocellular carcinoma, Cancer 89 (2000) 2274–2281.
[24] N. Mukaida, Y. Mahe, K. Matsushima, Cooperative interaction of nuclear factor-kappa B- and cis-regulatory enhancer binding protein-like factor binding elements in activating the interleukin-8 gene by pro-inflammatory cytokines, J. Biol. Chem. 265 (1990) 21128–21133.
[25] A. Takata, M. Otsuka, K. Kojima, T. Yoshikawa, T. Kishikawa, H. Yoshida, K. Koike, MicroRNA-22 and microRNA-140 suppress NF-κB activity by regulating the expression of NF-κB coactivators, Biochem. Biophys. Res. Commun. 411 (2011) 826–831.
[26] T. Block, A. Mehta, C. Fimmel, R. Jordan, Molecular viral oncology of hepatocellular carcinoma, Oncogene 22 (2003) 5093–5107.
[27] M. Karin, Nuclear factor-kappaB in cancer development and progression, Nature 441 (2006) 431–436.
[28] J. Ji, J. Shi, A. Budhu, Z. Yu, M. Forgues, S. Roessler, S. Ambs, Y. Chen, P. Meltzer, C. Croce, L. Qin, K. Man, C. Lo, J. Lee, I. Ng, J. Fan, Z. Tang, H. Sun, X. Wang, MicroRNA expression, survival, and response to interferon in liver cancer, N. Engl. J. Med. 361 (2009) 1437–1447.
[29] K. Kojima, A. Takata, C. Vadnais, M. Otsuka, T. Yoshikawa, M. Akanuma, Y. Kondo, Y.J. Kang, T. Kishikawa, N. Kato, Z. Xie, W.J. Zhang, H. Yoshida, M. Omata, A. Nepveu, K. Koike, MicroRNA122 is a key regulator of α-fetoprotein expression and influences the aggressiveness of hepatocellular carcinoma, Nat. Commun. 2 (2011) 338.
[30] M.S. Kumar, J. Lu, K.L. Mercer, T.R. Golub, T. Jacks, Impaired microRNA processing enhances cellular transformation and tumorigenesis, Nat. Genet. 39 (2007) 673–677.
[31] J. Lu, G. Getz, E.A. Miska, E. Alvarez-Saavedra, J. Lamb, D. Peck, A. Sweet-Cordero, B.L. Ebert, R.H. Mak, A.A. Ferrando, J.R. Downing, T. Jacks, H.R. Horvitz, T.R. Golub, MicroRNA expression profiles classify human cancers, Nature 435 (2005) 834–838.
[32] G. Martello, A. Rosato, F. Ferrari, A. Manfrin, M. Cordenonsi, S. Dupont, E. Enzo, V. Guzzardo, M. Rondina, T. Spruce, A. Parenti, M. Daidone, S. Bicciato, S. Piccolo, A MicroRNA targeting dicer for metastasis control, Cell 141 (2010) 1195–1207.

World Journal of Gastroenterology

Online Submissions: http://www.wjgnet.com/1007-9327office
wjg@wjgnet.com
doi:10.3748/wjg.v18.i12.1385

World J Gastroenterol 2012 March 28; 18(12): 1385-1390
ISSN 1007-9327 (print) ISSN 2219-2840 (online)

BRIEF ARTICLE

Assessment of disease progression in patients with transfusion-associated chronic hepatitis C using transient elastography

Ryota Masuzaki, Ryosuke Tateishi, Haruhiko Yoshida, Toru Arano, Koji Uchino, Kenichiro Enooku, Eriko Goto, Hayato Nakagawa, Yoshinari Asaoka, Yuji Kondo, Tadashi Goto, Hitoshi Ikeda, Shuichiro Shiina, Masao Omata, Kazuhiko Koike

Ryota Masuzaki, Ryosuke Tateishi, Haruhiko Yoshida, Toru Arano, Koji Uchino, Kenichiro Enooku, Eriko Goto, Hayato Nakagawa, Yoshinari Asaoka, Yuji Kondo, Tadashi Goto, Shuichiro Shiina, Kazuhiko Koike, Department of Gastroenterology, Graduate School of Medicine, The University of Tokyo, 1138655 Tokyo, Japan
Hitoshi Ikeda, Department of Clinical Laboratory, The University of Tokyo Hospital, 1138655 Tokyo, Japan
Masao Omata, Yamanashi Prefectural Hospital Organization, 4008506 Yamanashi, Japan
Author contributions: Masuzaki R, Tateishi R and Yoshida H designed research; Masuzaki R, Arano T, Uchino K, Enooku K, Goto E, Nakagawa H, Asaoka Y, Kondo Y and Goto T collected data; Tateishi R and Yoshida H analyzed data; Masuzaki R and Yoshida H wrote the paper; Tateishi R, Ikeda H and Shiina S reviewed the paper; Omata M and Koike K supervised the entire project.
Correspondence to: Dr. Ryota Masuzaki, Department of Gastroenterology, Graduate School of Medicine, The University of Tokyo, 7-3-1 Hongo, Bunkyo-ku, 113-8655 Tokyo, Japan. ryota-m@umin.net
Telephone: +81-3-38155411 Fax: +81-3-38140021
Received: May 12, 2011 Revised: August 1, 2011
Accepted: January 22, 2012
Published online: March 28, 2012

Abstract

AIM: To evaluate the relationship between liver stiffness and duration of infection in blood transfusion-associated hepatitis C virus (HCV) patients with or without hepatocellular carcinoma (HCC).

METHODS: Between December 2006 and June 2008, a total of 524 transfusion-associated HCV-RNA positive patients with or without HCC were enrolled. Liver stiffness was obtained noninvasively by using Fibroscan (Echosens, Paris, France). The date of blood transfusion was obtained by interview. Duration of infection was derived from the interval between the date of blood transfusion and the date of liver stiffness measurement (LSM). Patients were stratified into four groups based on the duration of infection (17-29 years; 30-39 years; 40-49 years; and 50-70 years). The difference in liver stiffness between patients with and without HCC was assessed in each group. Multiple linear regression analysis was used to determine the factors associated with liver stiffness.

RESULTS: A total of 524 patients underwent LSM. Eight patients were excluded because of unsuccessful measurements. Thus 516 patients were included in the current analysis (225 with HCC and 291 without). The patients were 244 men and 272 women, with a mean age of 67.8 ± 9.5 years. The median liver stiffness was 14.3 kPa (25.8 in HCC group and 7.6 in non-HCC group). The patients who developed HCC in short duration of infection were male dominant, having lower platelet count, with a history of heavier alcohol consumption, showing higher liver stiffness, and receiving blood transfusion at an old age. Liver stiffness was positively correlated with duration of infection in patients without HCC (r = 0.132, P = 0.024) but not in patients with HCC (r = -0.103, P = 0.123). Liver stiffness was significantly higher in patients with HCC than in those without in each duration group (P < 0.0001). The factors significantly associated with high liver stiffness in multiple regression were age at blood transfusion (P < 0.0001), duration of infection (P = 0.0015), and heavy alcohol consumption (P = 0.043)

CONCLUSION: Although liver stiffness gradually increases over time, HCC develops in patients with high stiffness value regardless of the duration of infection.

Key words: Transfusion-associated hepatitis C; Transient elastography; Hepatocellular carcinoma; Liver stiffness; Ultrasonography; Liver fibrosis

Peer reviewer: Sebastian Mueller, MD, PhD, Professor of Medicine, Department of Internal Medicine, Salem Medical Center, and Center for Alcohol Research, University of Heidelberg, Zeppelinstraße 11-33, Heidelberg 69121, Germany

Masuzaki R, Tateishi R, Yoshida H, Arano T, Uchino K, Enooku K, Goto E, Nakagawa H, Asaoka Y, Kondo Y, Goto T, Ikeda H, Shiina S, Omata M, Koike K. Assessment of disease progression in patients with transfusion-associated chronic hepatitis C using transient elastography. *World J Gastroenterol* 2012; 18(12): 1385-1390 Available from: URL: http://www.wjgnet.com/1007-9327/full/v18/i12/1385.htm DOI: http://dx.doi.org/10.3748/wjg.v18.i12.1385

INTRODUCTION

Hepatitis C virus (HCV) is a leading cause of chronic liver diseases, presenting serious public health problems worldwide[1,2]. HCV infection generally shows an asymptomatic onset and slow fibrosis progression, with cirrhosis developing after 20-50 years[3-7]. Progression of disease is known to depend on patients' characteristics at the onset of infection[8-12]. Infection at old age, male gender and heavy alcohol consumption are reported to be independently associated with rapid disease progression.

The onset of HCV infection can be reliably estimated in transfusion-associated chronic hepatitis C patients, in contrast to repeating injecting-drug users. In Japan, about 40% of chronic hepatitis C patients and HCV-related HCC patients have a history of blood transfusion typically in 1950s and 1960s[13], when blood supply depended on paid blood donors. Not a few of the blood donors were also injecting-drug users, mainly methamphetamine, among whom HCV spread first after the end of World War Ⅱ. Viral spread started to decline in Japan after commercial blood banks were entirely abolished in 1969[14].

Chronic hepatitis C with cirrhosis is a strong risk factor for hepatocellular carcinoma (HCC)[15,16]. It has been shown that the risk of HCC increases with the degree of liver fibrosis[17]. Until recently, however, the degree of liver fibrosis could be reliably assessed only with liver biopsy, an invasive procedure with the possibility of serious complications[18,19].

Liver stiffness, which can be noninvasively measured with transient elastography, has been recently reported to be well correlated with histologically assessed liver fibrosis stage[20]. We previously reported that liver stiffness is strongly associated with the risk of HCC[21,22]. The calculated stratum-specific likelihood ratio indicated that the post-test odds for the presence of HCC increase five-fold when liver stiffness is higher than 25 kPa and decrease to one-fifth when lower than 10 kPa. Furthermore, we have confirmed in a prospective study that liver stiffness is a significant risk factor for HCC development, together with male gender, clinical cirrhosis and serum albumin level. However, in those studies we did not fully consider the duration of HCV infection and the age at the onset of infection, which are indicated in several studies to be associated with disease progression.

The aim of this study is to evaluate the association between liver stiffness and the duration of infection in blood transfusion-associated hepatitis C patients with and without HCC, focusing on the risk of HCC development.

MATERIALS AND METHODS

Patients

This study conformed to the ethical guideline of the 1975 Helsinki Declaration and the ethical guidelines for epidemiologic research designed by Japanese Ministry of Education, Culture, Sports, Science and Technology and Ministry of Health, Labor and Welfare. The study design was approved by the ethics committee of the authors' institution. Between December 2006 and June 2008, a total of 1562 patients positive for HCV RNA visited the liver clinic of authors' institution. Among these patients, those with a history of receiving blood transfusion were consecutively enrolled (229 with HCC and 295 without). We excluded from the present study those patients with concomitant hepatitis B virus surface antigen positivity, patients with uncontrollable ascites, patients on interferon therapy, and patients who received multiple blood transfusions.

Transient elastography

Liver stiffness was obtained noninvasively by using Fibroscan (Echosens, Paris, France), a newly developed medical device based on elastometry. Liver stiffness measurement (LSM) was considered valid only when at least eight acquisitions were successful with a success rate of at least 60% and the ratio of inter-quartile range (IQR) to the median value was larger than 30%.

Diagnosis of hepatocellular carcinoma

In patients with HCC, the cancer was diagnosed by dynamic computed tomography (CT), where intrahepatic nodules with hyperattenuation in the arterial phase with washout in the late phase were considered as definite HCC[23,24]. Histopathological diagnosis, using ultrasound-guided biopsy samples, was also performed when required. In patients without HCC, the cancer was ruled out by ultrasonography. No HCC was detected in the subsequent six-month follow-up period among these patients.

Laboratory tests

We determined the following parameters on the day of LSM: serum albumin and total bilirubin concentrations, serum aspartate aminotransferase (AST) and alanine aminotransferase (ALT) levels, prothrombin activity and platelet count. Serogrouping of HCV was assessed by enzyme-linked immunosorbent assay (ELISA) (Immucheck F-HCV Gr Kokusai; Sysmex, Kobe, Japan)[25]. Based on the prevalence of each HCV genotype in Japan, serogroup 1 was assumed to represent genotype 1b and serogroup 2 to represent genotype 2a or 2b.

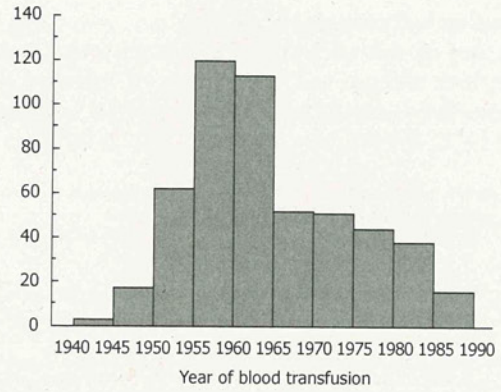

Figure 1 Frequency distribution of the year of receiving blood transfusion among the subjects. There is a peak around the year 1960.

Table 1 Characteristics of patients according to presence of hepatocellular carcinoma *n* (%)

Characteristics	HCC	Non-HCC	*P* value
Overall patients	*n* = 225	*n* = 291	
Gender (M/F)	126/99	118/173	0.0005
Age (yr)[1]	71.2 (66.1-75.7)	68.1 (58.7-72.4)	< 0.0001
Platelet count (10^9/L)[1]	95 (74-133)	161 (111-200)	< 0.0001
ALT (IU/L)[1]	48 (34-68)	42 (25-69)	0.006
Alcohol consumption > 50 g/d	51 (22.7)	28 (9.6)	< 0.0001
Liver stiffness (kPa)[1]	25.8 (17.3-37.4)	7.6 (5.6-13.9)	< 0.0001
IQR (kPa)[1]	4.0 (2.5-6.0)	1.6 (1.2-2.6)	< 0.0001
Duration (17-29 yr)	*n* = 34	*n* = 64	
Gender (M/F)	25/9	38/26	0.0028
Age (yr)[1]	73.1 (65.7-77.1)	59.7 (47.2-69.2)	0.033
Platelet count (10^9/L)[1]	95 (76-154)	180 (116-229)	< 0.0001
ALT (IU/L)[1]	51 (34-89)	42 (22-77)	0.2071
Alcohol consumption > 50 g/d	12 (35.3)	9 (14.1)	0.023
Liver stiffness (kPa)[1]	26.1 (16.8-53.3)	5.9 (4.9-12.1)	< 0.0001
Duration (30-39 yr)	*n* = 40	*n* = 59	
Gender (M/F)	16/24	23/36	0.9191
Age (yr)[1]	72.0 (65.4-76.7)	62.3 (55.7-68.6)	< 0.0001
Platelet count (10^9/L)[1]	93 (68-120)	151 (97-215)	< 0.0001
ALT (IU/L)[1]	42 (33-65)	48 (27-80)	0.7591
Alcohol consumption > 50 g/d	6 (15)	7 (11.9)	0.7641
Liver stiffness (kPa)[1]	28.7 (20.1-37.8)	7.4 (5.7-13.8)	< 0.0001
Duration (40-49 yr)	*n* = 101	*n* = 127	
Gender (M/F)	58/43	51/76	0.0113
Age (yr)[1]	69.2 (65.8-73.6)	69.9 (65.7-72.7)	0.8107
Platelet count (10^9/L)[1]	97 (67-136)	163 (112-195)	< 0.0001
ALT (IU/L)[1]	48 (34-69)	38 (23-64)	0.0080
Alcohol consumption > 50 g/d	25 (24.8)	8 (6.3)	0.0001
Liver stiffness (kPa)[1]	25.1 (17.5-37.4)	8.2 (5.8-14.1)	< 0.0001
Duration (50-70 yr)	*n* = 50	*n* = 41	
Gender (M/F)	27/23	18/23	0.4016
Age (yr)[1]	74.4 (70.0-78.1)	73.7 (66.3-79.2)	0.5658
Platelet count (10^9/L)[1]	97 (81-141)	147 (117-189)	0.0001
ALT (IU/L)[1]	52 (36-69)	46 (32-63)	0.1700
Alcohol consumption > 50 g/d	8 (16)	4 (9.8)	0.5363
Liver stiffness (kPa)[1]	16.0 (8.0-36.3)	7.9 (6.5-15.8)	< 0.0001

[1]Data are expressed as median (25th-75th percentiles). ALT: Alanine aminotransferase; IQR: Inter-quartile range; HCC: Hepatocellular carcinoma; M: Male; F: Female.

Duration of infection and liver stiffness progression

The date of blood transfusion was obtained by interview. Duration of infection was derived from the interval between the date of blood transfusion and the date of LSM. The rate of liver stiffness progression was calculated as follows: present liver stiffness-minimal stiffness value in the cohort (kPa)/interval after blood transfusion (years).

Statistical analysis

Data were expressed as median and 25th-75th percentiles in parenthesis unless otherwise indicated. The categorical variables were compared by χ^2 tests, whereas continuous variables were compared with unpaired Student's *t* test (parametric) or Mann-Whitney *U* test (non-parametric). A *P* value < 0.05 on two-tailed test was considered significant.

The correlation between liver stiffness and the interval from blood transfusion was assessed by Spearman's rank correlation. The duration of infection was arbitrarily stratified into 4 groups, 17-29 years; 30-39 years; 40-49 years; and 50-70 years. The difference in liver stiffness according to the presence of HCC was assessed in each group. Multiple linear regression analysis was used to determine the factors associated with liver stiffness. Processing and analysis were performed by using the S-plus Version 7 (TIBCO Software Inc., Palo Alto, CA, United States).

RESULTS

Patients' profile

A total of 524 patients underwent LSM. Eight patients were excluded because of unsuccessful measurements, mostly due to obesity (four patients had IQR/median > 30% and four had a success rate lower than 60%). Thus 516 patients were included in the current analysis (225 with HCC and 291 without). Their characteristics at the time of LSM are summarized in Table 1. The patients were 244 men and 272 women, with a mean age of 67.8 ± 9.5 years. The median liver stiffness was 14.3 kPa (25.8 in HCC group and 7.6 in non-HCC group). Figure 1 shows the frequency distribution of the year of receiving blood transfusion among the subjects. A peak is noted around the year 1960.

Characteristics of patients according to the duration of infection

Characteristics of patients were compared between patients with and without HCC in each duration of infection group (Table 1). The patients who developed HCC in short duration of infection were male dominant, having low platelet count, with a history of heavier alcohol consumption, showing higher liver stiffness, and receiving blood transfusion at an older age.

Correlation between liver stiffness and duration of infection

The correlation between liver stiffness and duration of